

# **APPROACH FOR STRUCTURALLY CLEARING AN ADAPTIVE COMPLIANT TRAILING EDGE FLAP FOR FLIGHT**

Eric J. Miller, William A. Lokos, Josue Cruz, Glen Crampton, Craig A. Stephens  
NASA Armstrong Flight Research Center, Edwards, California, 93523

Sridhar Kota, Gregory Ervin  
FlexSys Inc., Ann Arbor, Michigan 48105

Pete Flick  
AFRL Air Vehicles Directorate, Wright-Patterson Air Force Base, Ohio, 45433

## **1. ABSTRACT**

The Adaptive Compliant Trailing Edge (ACTE) flap was flown on the National Aeronautics and Space Administration (NASA) Gulfstream GIII testbed at the NASA Armstrong Flight Research Center. This smoothly curving flap replaced the existing Fowler flaps creating a seamless control surface. This compliant structure, developed by FlexSys Inc. in partnership with the Air Force Research Laboratory, supported NASA objectives for airframe structural noise reduction, aerodynamic efficiency, and wing weight reduction through gust load alleviation. A thorough structures airworthiness approach was developed to move this project safely to flight. A combination of industry and NASA standard practice require various structural analyses, ground testing, and health monitoring techniques for showing an airworthy structure. This paper provides an overview of compliant structures design, the structural ground testing leading up to flight, and the flight envelope expansion and monitoring strategy. Flight data will be presented, and lessons learned along the way will be highlighted.

## **2. ACRONYMS**

ACTE	= Adaptive Compliant Trailing Edge
AFRC	= Armstrong Flight Research Center
AFRL	= Air Force Research Laboratory
AGPS	= Aerodynamic Grid and Paneling System
AOA	= angle of attack
DLL	= design limit load
FAR	= Federal Aviation Regulations
FEM	= finite element method
FLL	= Flight Loads Lab
FOS	= factor of safety
GIII	= Gulfstream III
GVT	= ground vibration test
IBTS	= inboard transition section
MAW	= Mission Adaptive Wing
NASA	= National Aeronautics and Space Administration
NDI	= non-destructive inspection

OBTS = outboard transition section  
RBS = rear beam station  
SCRAT = Subsonic Research Aircraft Testbed  
SHSS = steady heading side slip  
TRL = technology readiness level

### 3. INTRODUCTION

Flight-testing new and innovative structures in a flight-relevant environment promotes the transition of structural technologies from research to mainstream production. Wind-tunnel and ground-based load testing of structural flight technologies have inherent limitations that can be overcome through flight-testing. The National Aeronautics and Space Administration (NASA) Armstrong Flight Research Center (AFRC) (Edwards, California) has procured, modified, and instrumented a Gulfstream GIII airplane (Gulfstream Aerospace Corporation, Savannah, Georgia) to increase the technology readiness level (TRL) of promising new flight technologies. This airplane is named the Subsonic Research Aircraft Testbed (SCRAT).<sup>1</sup>

The NASA AFRC partnered with the Air Force Research Laboratory (AFRL) and FlexSys Inc. (Ann Arbor, Michigan) to flight-test the Adaptive Compliant Trailing Edge (ACTE) experiment to demonstrate a seamless adaptive compliant structural control surface in flight. Wind-tunnel testing and small-scale flight tests of the compliant technology were conducted as a first step, but a full-scale compliant structure requires flight-testing to build confidence before the technology can be fully transitioned to commercial industry.<sup>2</sup>

Since the Mission Adaptive Wing (MAW) program in the 1980s demonstrated the benefits of seamless, morphing, wing leading, and trailing edges on a modified F-111; many in the aviation research and development community have attempted to realize those benefits without the associated weight and complexity of the mechanism behind MAW.<sup>3</sup>

Structural design optimization methods that produce a design for a structure that can bend and twist to achieve various wing shapes for optimum flight over the envelope are the key enabler for ACTE. The ACTE is envisioned as a multifunctional aerodynamic surface that enables the airfoil shape to be optimized for minimum drag over a broad range of flight conditions, instead of a single flight condition in traditional wing design. The ACTE can also be actuated at high enough rates to enable structural load alleviation during maneuvers and gusts, leading to lighter weight wing structures and more efficient aerodynamic vehicle configurations. The ACTE can also achieve large deflections for use in high lift conditions.

Contemporary aviation structures employ a system of mechanisms to mechanically actuate control surfaces. FlexSys technology takes advantage of material elasticity to produce large structural deformations while maintaining the structural strength required to carry the air loads.

Two ACTE flaps were fabricated and assembled to replace both existing Fowler flaps on the SCRAT. Figure 1 shows a photograph of the SCRAT with installed ACTE flaps. The objective of the flight-test program was structural flight demonstration of the ACTE technology. The ACTE flaps were fixed at a predetermined deflection angle for each flight and remained fixed in that position for the duration of the flight. The flight-test deflection range of the ACTE was  $-2^{\circ}$

and  $+30^\circ$  (- signifies up flap deflections, + signifies down flap deflections) while the ACTE was designed and operated to  $-9^\circ$  and  $+40^\circ$  on the ground.



Figure 1. ACTE installed on the GIII at a flap deflection of  $20^\circ$ .

#### 4. COMPLIANT DESIGN

Comparing human-engineered machines to those found in nature, we see fundamental differences in how they are made, work, and perform. Most engineered systems that transmit mechanical motions or forces or energy comprise a plurality of rigid components connected by various interfaces or joints. Engineered artifacts, such as engines, pumps, propellers, wings et cetera, have fixed geometry optimized for peak performance at a specific operating condition. Designs in nature, from tree branches, bird wings, elephant trunks, and invertebrates which account for a majority of all living creatures are suitably compliant (flexible), comparatively strong, and offer a tremendous range of shape adaptation to dynamically maximize their performance.

Compliant design<sup>4</sup> embraces elasticity, rather than avoiding it, to create one-piece kinematic machines or joint-less mechanisms that are strong and flexible (for shape adaptation). In common flexural joints or flexures are concentrated at localized zones, sometimes along a single axis, surrounded by relatively rigid sections. These zones of high stress concentration limit the load-carrying capacity of systems with flexural joints. Distributed compliance is the ability of a structural system to be simultaneously flexible and strong; two quantities that are usually considered antithetical in traditional engineering. Designs with distributed compliance exhibit both strength and flexibility since every section of the material participates in both load-sharing and kinematic functions. The cascading benefits of elastic design are many: high fatigue life, significant reduction in parts, and mechanical complexity. Elimination of joints improves precision and eliminates friction and wear.

The concept of distributed compliance and associated design methods were developed by Sridhar Kota, University of Michigan. By combining the principles of continuum mechanics and kinematics FlexSys Inc. developed algorithms for synthesizing lightweight compliant structures that have high (static and fatigue) strength and sufficiently flexible to deliver a desired kinematic or shape-morphing function.<sup>5</sup>

The compliant iris mechanism developed by FlexSys Inc. shown in figure 2 below demonstrates the concept of distributed compliance. The actuation energy supplied by simply rotating the external tabs (one clockwise, the other counterclockwise) is distributed more or less uniformly as strain energy. Large deformations can be achieved by subjecting every section of the material to contribute equally to the (shape morphing) objective while all components share the loads. Therefore, every section of the material undergoes only very small linear elastic strain with very low stress, and hence the structure can undergo large deformations with high fatigue life.



Figure 2. Compliant mechanism example.

The design of FlexFoil™ ACTE is based on these principles of compliant design. ACTE distributes compliance throughout the structure, changing the wing camber from  $-9^\circ$  to  $+40^\circ$  on demand, while sustaining the required external load. The FlexFoil™ variable geometry surface uses the natural flexibility of aerospace-grade materials arranged in a joint-less skeletal configuration to continuously reshape its external form by internal actuators. Each section of the internal compliant structure is optimized to share the external load and undergoes specified deformation without overstressing any part of it. This distributed compliance enables large deformations with very low stresses so that the system can be cycled thousands of times without failure (high fatigue life).

## 5. STRUCTURAL DEMONSTRATION OBJECTIVES

The ACTE design flight envelope was based upon the GIII Fowler flap operational envelope. The goal for the ACTE test program was to push out to the limits of the GIII testbed which determined the additional flap settings and airspeed limits. Demonstrating the ACTE technology within the envelope applicable to cruise drag reduction and gust load alleviation was deemed an additional requirement of this test program for showing the versatility of this technology.

Even though the ACTE structure was designed for a flap deflection range up to  $+40^\circ$  down, the flight demonstration was held to a maximum deflection of  $+30^\circ$  because the flap would be exposed to fully separated flow at that point. The up-flap deflections were capable of  $-9^\circ$ , but were limited to  $-2^\circ$  due to the takeoff restrictions of the GIII. Table 1 shows the Fowler flap and

ACTE operational and design airspeeds. The design airspeeds were derived from the Federal Aviation Requirements (FAR) which required an additional 15-knot head-on-gust condition to be added to the airspeed operational limit. Figure 3 shows the design envelopes for the specific ACTE flap deflections along with the maneuver test points. Research test points were distributed over the envelope for collecting steady state trim points and maneuvering data for each flap deflection. Loads points at 10,000-ft altitude and Mach 0.3, 0.4, and 0.5 were added in for assessing the individual flap deflections against each other at a consistent dynamic pressure.

Table 1. GIII Fowler flap and ACTE operational and design airspeeds.

GIII Fowler flap position degrees	ACTE flap position degrees	Airspeed operational limit knots	Design airspeeds (+15 knot gust) knots
0	2	340	355
0	5	300	315
10	15	250	265
39	30	170	185

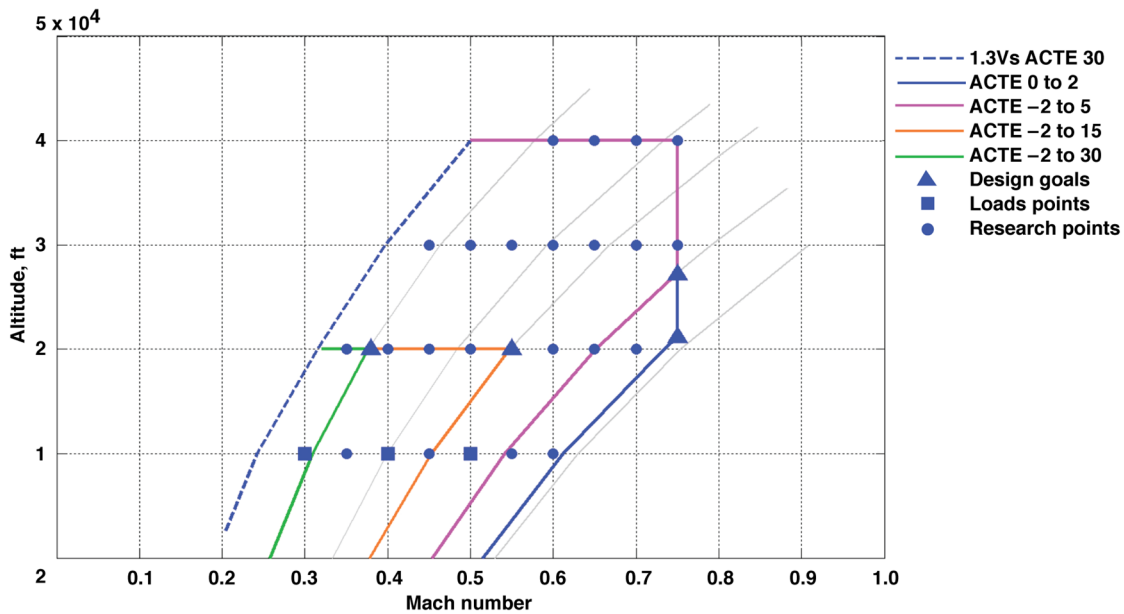


Figure 3. ACTE flight envelope and test conditions.

## 6. INTERFACE GEOMETRY DEFINITION

Defining the correct interface to the GIII flap attachment points was required to produce a seamless blending of the flap and wing surfaces. The integration of the ACTE on to the GIII required removal of the Fowler flap, flap tracks, flap actuators, and flight and ground spoilers. The goal of the ACTE integration was to match the shape of the existing Fowler flap in its zero-degree flap deflection fully retracted state. The second goal was to integrate the ACTE onto the GIII with as little modification to the GIII as possible. The main boundaries consisted of the wing cove aft of the rear spar and inboard and outboard wing trailing edge sections which are

shown in figure 4. The wing cove keep-out area was defined by a plane intersecting the upper and lower trailing edge wing skins. All ACTE structure was required to stay out of this area. The aft wing cove contained hydraulic lines, an aileron cable, and spoiler actuation hardware. Due to ease of integration and maintaining airplane functionality, a large portion of the hardware in the cove was left un-modified.

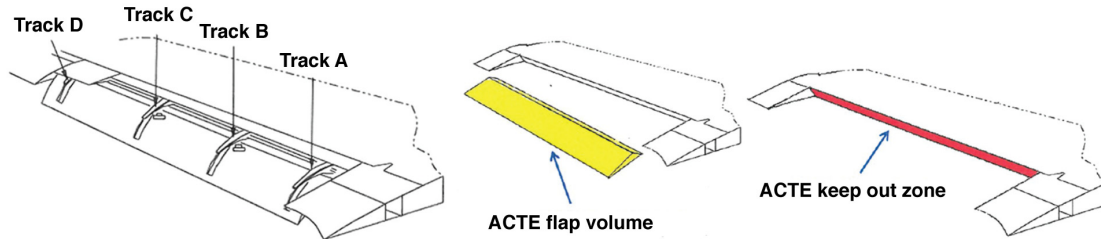


Figure 4. ACTE structural design interfaces.

Ideally, the ACTE compliant structure would have attached directly to the GIII wing rear spar, but due to the keep-out zone requirements, a secondary spar located aft of the GIII rear spar was designed and fabricated to minimize modifications to the aircraft. Figure 5 highlights the interface components between the rear spar and the secondary spar of the ACTE structure. The ACTE was attached to the rear spar using existing Fowler flap track fitting attachment points. New modified flap track interface fittings were designed and fabricated to attach the ACTE flap to the wing. The fittings were fabricated using 4340 steel heat treated to 200ksi. The original Fowler flaps were designed to carry normal force and bending moment loads at tracks B and C and only normal force loads at tracks A and D. The four Fowler flap attachment points are labeled in figure 4. The same naming scheme was used for the ACTE attachment points. All four ACTE interface fittings were designed to carry both normal force and bending moment at each fitting. The lateral loads on the original Fowler flap were reacted out at track D which is adjacent to the aileron. A similar reaction structure at track D was created for ACTE to react the flap lateral loads. The ACTE compliant structure was separated into three main components as shown in figure 6. The main flap, which was the main lifting surface, and two transition structures were used to blend the flap surface into the fixed wing inboard and outboard trailing edge sections.

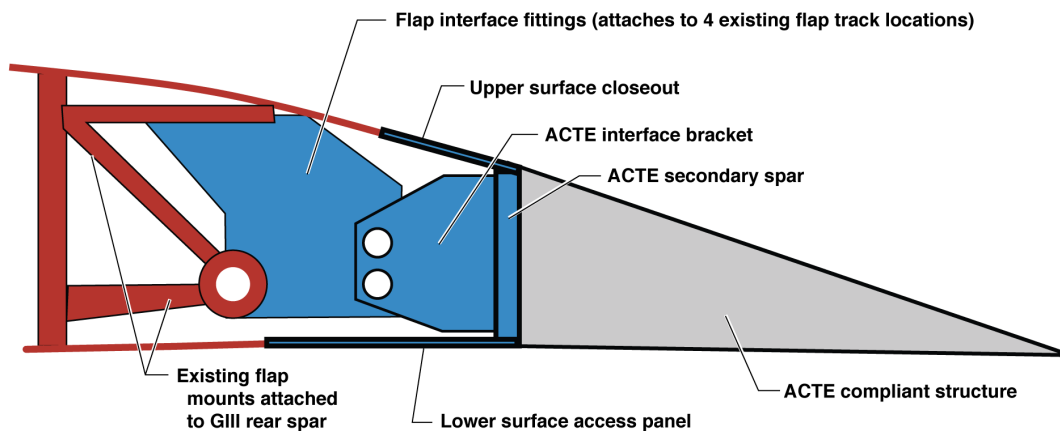


Figure 5. ACTE interface components (representative cross section).

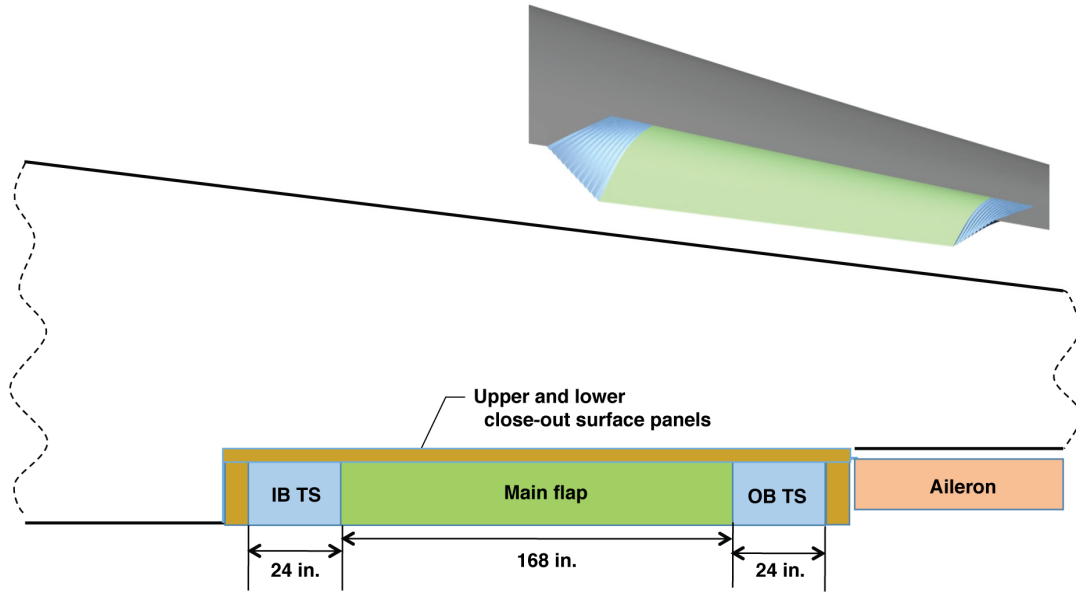


Figure 6. ACTE structural components.

## 7. STRUCTURE DESIGN AND ANALYSIS REQUIREMENTS

NASA AFRC has a long history of flight testing new and innovative structures in-flight. Guidelines for structural design and analysis have been developed from this experience and were applied to the ACTE project. The structure analysis factor of safety (FOS) is probably the most important design requirement and using an improper value can have ramifications with regard to aircraft safety and or excessive weight. The common industry standard for FOS is 1.5 on design limit load (DLL), but that applies to a production structure that is adequately instrumented and proof tested to failure. Due to project schedule and budget constraints the ACTE project modified the airworthiness approach to best meet the project objectives. For unique one-of-a-kind experiments where weight savings is not necessarily the prime objective, higher FOS should be used. Typically the scheme for most projects at AFRC is to use higher factors of safety for structures that do not require the weight savings. The FOS used for the ACTE project are shown in table 2.

Table 2. ACTE structure analysis FOS.

Structural component	FOS on DLL
Interface attachment structure	2.25
Compliant structure	2.0
Actuation mechanism	3.0

The interface attachment structure used a FOS of 2.25 and consists of the interface fittings, simulated spar structure, and closeout panels that attach and blend the compliant ACTE structure to the wing. The FOS of 2.25 was probably excessive regarding some parts of the structure, and it is the authors' opinion that the project should have targeted something lower in the secondary structure areas. Using a lower factor of safety would have reduced the flap weight which in turn

would have decreased the inertial effects in the flight data. The compliant mechanism, which is the heart of the technology demonstration, was designed to a FOS of 2.0 due to the uniqueness of the structure. Typical past projects have used FOS between 1.5 and 2.0 for structural demonstrations, and this flight project confirmed that range; a FOS between 1.5 and 2.0 is probably about right. The actuation drive hardware of the flap was designed to 3.0, which in practice, was an appropriate choice. Due to the nature of this flap and given that the flap angle was fixed on the ground before flight, the abuse loads were actually a bigger driver than loads observed in-flight. The chosen FOS were conservative because weight and size were not important design constraints. Eventually the factors could be reduced for production hardware.

The required envelope for the ACTE flights extends up to 40,000 ft. The temperature on the flap surface was recorded at -50°F on multiple flights. AFRC guidelines require a design/test temperature range of -65 to 160°F and ACTE met those design requirements.

## **8. LOAD AND STRESS ANALYSIS APPROACH**

The ACTE design envelope was shown in figure 3. The inertial normal acceleration of 0 to 2g for the Fowler flap operating envelope was used for the design of the ACTE. The load prediction scheme considered combinations of maximum flap angle, maximum dynamic pressure, and inertial loads. The FARs require that trailing-edge flaps be designed to a head-on gust condition of a max speed plus 15 knots, and this 15 knot head on the gust load case resulted in the highest flap loads for the analysis. The external pressure and inertial loads were derived by AFRC and delivered to FlexSys Inc. for design and analysis of the flap.

Computational analysis was used to determine the pressure loads acting on the wing. Pressure load models were generated for two separate computational codes. The code selected for each analysis point was based on which available tool would be most accurate at the flight conditions in question.

For some analysis cases, a panel code called CMARC (Aerologic, Los Angeles, California)<sup>6</sup> was used. This code is quick and accurate for pre-stall, low subsonic flow. Generated by a gridding utility called LOFTSMAN (Aerologic, Los Angeles, California), the CMARC model consists of a coarse structured grid that contains the fuselage, wing, and vertical and horizontal tails. A separate grid is created for each ACTE flap deflection, for a total of 6 different grids. Additionally, the aileron control surface is modeled as a physical change to the geometry and the grid of the wing. The elevator control surface is modeled through the use of transpiration and does not require re-gridding. An example CMARC grid for 30° flap deflection is shown as the left hand side of figure 7.

A higher fidelity analysis approach was taken for most cases (ACTE -2° through +15°). TRANAIR (Calmar Research Corporation, Needham, Massachusetts)<sup>7</sup> is a non-linear full potential solver directly coupled with an integral boundary layer solver. Aerodynamic Grid and Paneling System (AGPS) was used to generate the surface grid representation of the GIII aircraft with the ACTE. The TRANAIR structured surface grid is more detailed than the CMARC grid; and it models the fuselage, wing, vertical and horizontal tails, engine, and engine pylon. A separate grid was created for each ACTE flap deflection, for a total of six different grids. For TRANAIR, both the elevator control surface and aileron are modeled through the use of



transpiration. An example TRANAIR surface grid for 30° flap deflection is shown as the right hand side of figure 7.

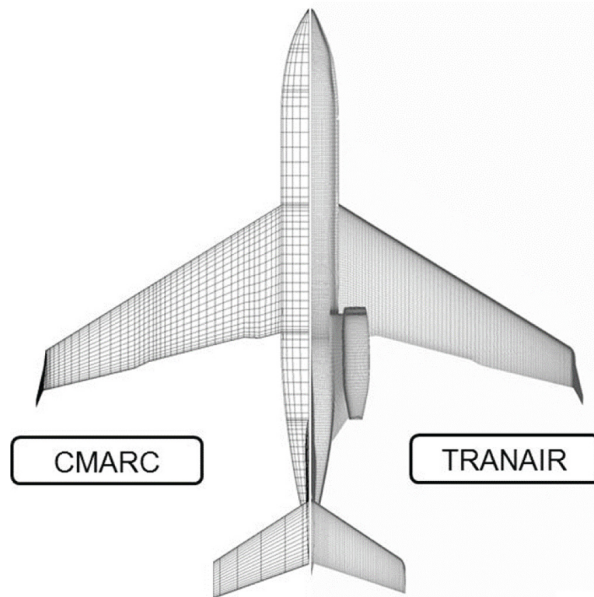


Figure 7. Computational grids for CMARC (left) and TRANAIR (right).

There are some limitations with both the CMARC and TRANAIR models. Neither CMARC nor TRANAIR can handle large amounts of flow separation. Flow separation on the flap is not a concern at 5° ACTE deflection or below, but separation becomes more probable at 15°- and 30°- ACTE deflection.

The external loads were used for determining the internal structural loads and deriving final structural margins. The stress analysis used a combination of hand calculations and finite element method (FEM) models to validate positive margins on all the structural components. A complete shell FEM model was used for deriving the component loads, and hand calculations were used for demonstrating positive margin on each component or fastener. The FEM analysis was completed using commercial off-the-shelf codes of Nastran<sup>8</sup> and ANSYS<sup>9</sup>.

The main FEM components are highlighted in figure 8. There were two main load cases that apply to the flaps in flight. The first includes pressure cases which were derived from the different flap deflections and corresponding flight conditions. The second case is the interaction between the ACTE structure and GIII wing structure. The magnitudes of the loads are related to the general stiffness of both structures. The interface loads are increased as the airplane load factor increases causing higher deflections in the wing.

The GIII Fowler flap was designed so that all lateral side loads on the fowler flap are reacted into the outboard flap track D. The same approach is taken for the ACTE interface fitting D. The fitting D lateral support structure is made up of the interface fitting D, an upper skin close out, a lower skin stiffener, an internal stiffener outboard of the fitting, and inboard and outboard clips for tying into the wing structure. The lateral force is reacted into the forward interface fitting

spherical bearing. The lateral force component is reacted out of the interface fitting through the upper and lower skins attached to the flanges of the interface fitting. Using applied loads from the ACTE and skin pressure loads, the loads on each component and fastener were calculated from the FEM model.

As it turned out, the external loads were found to have been over predicted which resulted in the structural margins being more positive than originally planned. The main reason of the over predicted loads was the use of rigid aerodynamic loading analysis. The aforementioned method does not include the aeroelastic effects that the aircraft experiences in flight. The wing deformation due to aerodynamic and inertial loading will modify the pressure distribution and in turn modify the loads on the wing. As a result the external loads analysis was conservative.

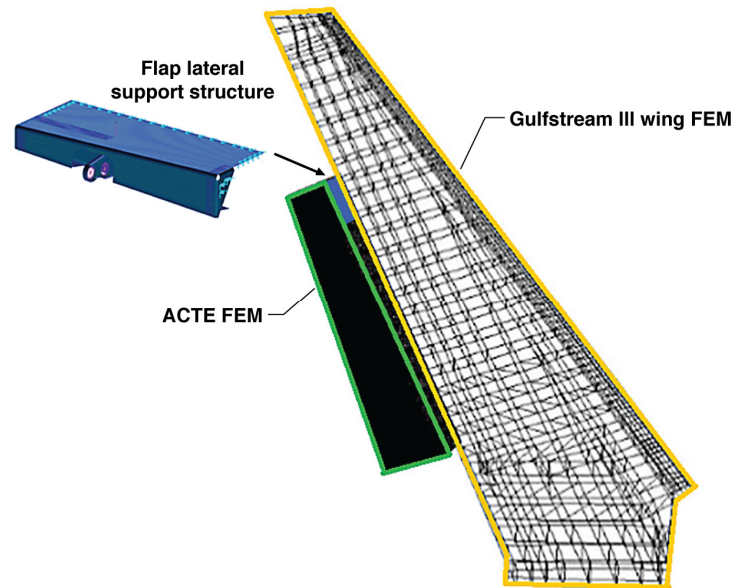


Figure 8. ACTE FEM analysis components.

## 9. GROUND TESTING APPROACH

The ACTE project used a building block approach to gain confidence in the structure before committing to the final flight articles. A schematic of the building block approach is shown in figure 9. System material characterization verified material properties and allowables for analysis. The ACTE control surfaces were subjected to various rigorous tests including life cycle fatigue, GVT, temperature variations (-65°F to 180°F), and exposure to chemicals and UV radiation. Sub-component prototypes were built to verify that the structure behaved as expected and would meet the operational load and fatigue requirements. The prototypes were proof tested using external loads applied with bonded load pads. The applied loads were distributed to match the expected in-flight pressure loading. A number of the prototypes were taken to failure which demonstrated the external load margin was more than adequate. The failure testing also gave insight into the behavior and weak spots for the flight articles. The fatigue testing was required to show the structure was good for a minimum of 1,000 deflection cycles using a scatter factor of 4.0. The prototype structures show no degradation during the fatigue testing. The prototypes

were instrumented with strain sensors and compared against the FEM models. This incremental approach was able to uncover minor issues such as problems that would arise during manufacturing of the full-scale articles before they manifested themselves in the final flight articles. A final operational/qualification test was conducted on the flight articles as a final checkout of the fabrication workmanship and FEM model correlation to verify everything was working as expected. The operational/qualification tests were very beneficial for getting a feel for the flap characteristics and working out kinks in the instrumentation before flight.

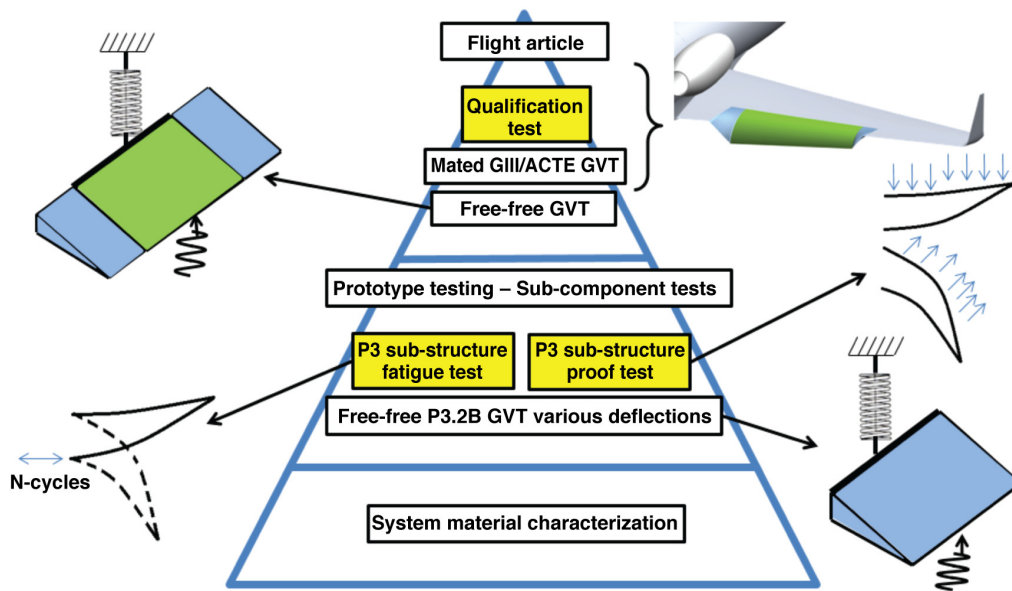


Figure 9. ACTE building block testing approach.

## 10. INSTRUMENTATION AND MONITORING OVERVIEW

The ACTE project flew beyond the cleared Fowler flap flight operational envelope as shown in table 1 and therefore monitoring for overloads during the flight envelope expansion was a significant risk reduction element of conducting a safe flight project. External load predictions indicated possible strength exceedances of the wing box during high-dynamic-pressure maneuvers. The ACTE flap and attachment hardware could also have approached or exceeded the structural limits of the wing rear spar interface attachment. Given that the ACTE flight-test article was a new and unique one-of-a-kind flight structure with no existing flight history, it was important to understand what was going on in the structure in-flight. Understanding the structural strains and loads in direct loads paths is a key element of any airworthiness plan as the flight envelope is expanded.

The ACTE and wing box structure were instrumented at multiple locations for the monitoring of overloads during flight-testing. Figure 10 shows the locations of the two instrumented wing rear beam stations (RBS) and the four instrumented wing interface fittings on the left wing. Fittings were instrumented on both wings for flight-testing. The two wing RBSs were instrumented for monitoring normal force, bending moment, and torque wing loads at the 40% chord reference line; the four wing interface fittings were monitored for combinations of flap normal force,

bending moment, and lateral side load. The side load was monitored at the outboard interface fitting (D) which was the only interface that transmits side load from the flap to the wing box. Both the left and right ACTE structures were instrumented symmetrically, allowing the team to observe any asymmetric loading during flight-test points. A number of thermocouples were added to the left wing to observe skin temperature and correct strain instrumentation for thermal effects. Fiber optic strain sensors were also used extensively on both flaps to understand how the strains varied throughout the structure. Table 3 shows the total number of installed sensors for ACTE.

Table 3. ACTE instrumentation sensor count and load equation errors.

Structures parameters	Number of sensors	Equation errors
Wing loads	32	RBS 152: 2% RBS 343: 5%
Interface normal force and bending moment loads	21	Normal force: 10% Bending moment: 5%
Cartridge side load	4	5%
Metallic load/strain sensors located on ACTE	43	1%
Cartridge strain (fiber)	6000	NA
Vertical tail force	Derived from airspeed, aircraft sideslip angle, and rudder position	NA
Temperature	8	NA

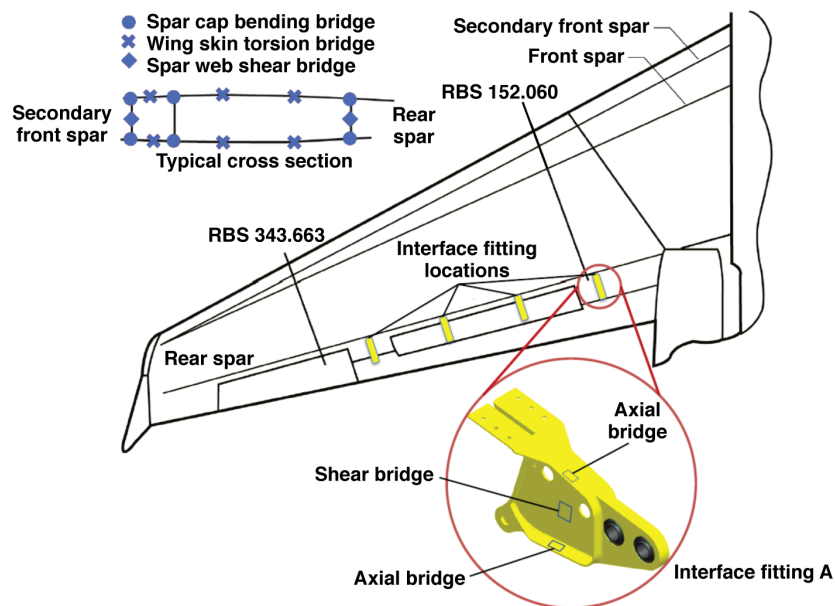


Figure 10. ACTE wing and interface instrumentation.

## 10.1 Wing load instrumentation and monitoring

Wing load predictions with the ACTE flap installed indicated the potential for approaching or exceeding the load limits at two wing stations. In preparation for the flight test of the new flap those two stations were instrumented with a total of 16 metallic foil strain gages as shown in figure 10. In order to produce the required multi-gage load equations to utilize those new strain signals a ground loads calibration test effort was undertaken. The testing was conducted in the NASA Armstrong Flight Loads Lab (FLL). The load calibration testing involved the application of a family of known load cases with the aircraft in two different support configurations.<sup>10</sup> There were a total of 16 independent hydraulic jack load stations. Both hydraulic loading and shot bags were used in some load cases. For some of the load cases the aircraft was partially supported by airbags, as shown in figure 11. The airbag testing operation was done to isolate the effect on the wing box strains due to variations in main landing gear loads.

Multi-gage load equations were derived, using the ground test data, and used real time to provide wing normal force, bending moment, and torque load data that was compared against the strength limits for the two measurement stations. Typical inboard station wing loads data are shown in figures 12 and 13 for various ACTE flap deflections. As the ACTE flap deflection was increased, higher normal force, bending moment, and torque loads were observed in the inboard wing station. Monitoring these load signals allowed the safe expansion of the flight envelope while using the experimental flap. Highest loads observed during the ACTE flights were on the order of 50% of design limit loads. The ground load testing yielded accurate load equations and provided a good training opportunity. The wing load calibration testing provided insight into the structure that the author believes is valuable even though the loads observed in flight turned out to be relatively low.



Figure 11. Photograph of hydraulic up load case with aircraft supported on airbags.

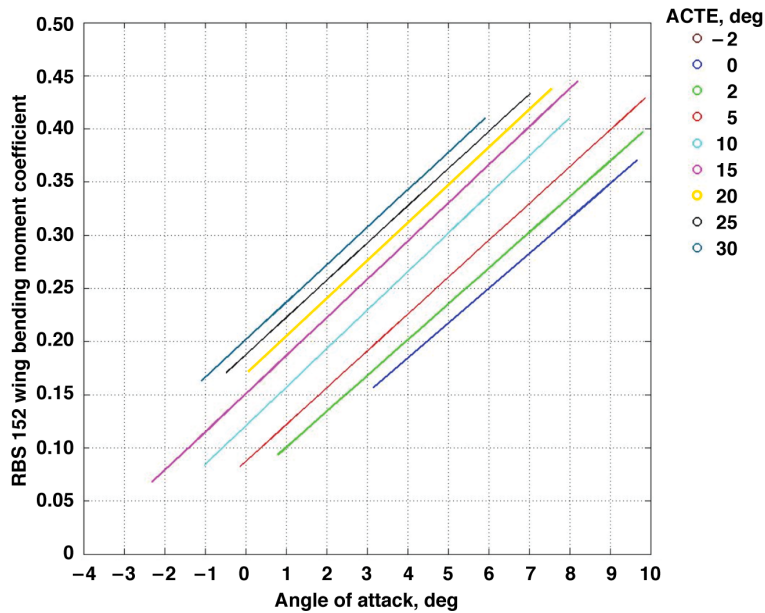


Figure 12. RBS152 wing bending moment loads for ACTE flap deflections.

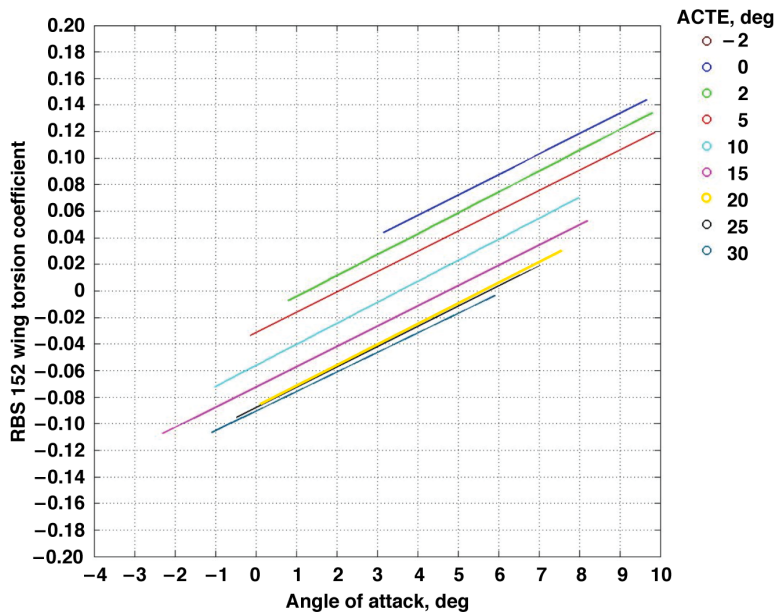


Figure 13. RBS152 wing torque for ACTE flap deflections.

## 10.2 Interface load instrumentation and monitoring

The four interface fittings on both flaps were instrumented to monitor normal force and bending moment (hinge) loads.<sup>11</sup> A combination of axial, bending, and shear metallic strain gage bridges were installed on all eight interface fittings. The four individual interface fittings with installed instrumentation are shown in figure 14. Each individual interface fitting was calibrated in a ground fixture off of the airplane. The applied loads were a combination of normal force,

bending moment, and axial drag loads. The applied loads were scaled for each fitting depending on its design strength limits. Interface fittings B and C had higher limits than fittings A and D.



Figure 14. ACTE interface fitting strain gage installation.

Due to the short nature of these fittings, the calibration was challenging to get an adequate amount of response out of the bridge to derive load equations. It is recommended for future projects of this nature that the fittings be optimized structurally for producing more response in addition to adding more strain gages to increase strain gage response output. The total combined interface fitting normal force and hinge moment load coefficients for multiple flap deflections are shown in figures 15 and 16 below.

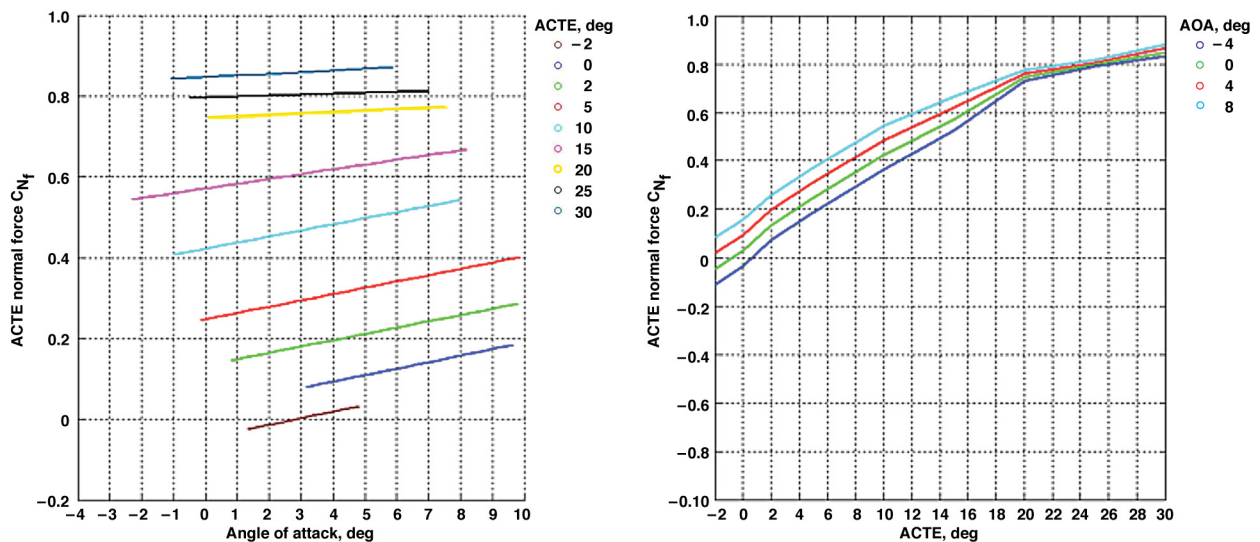


Figure 15. ACTE interface normal force.

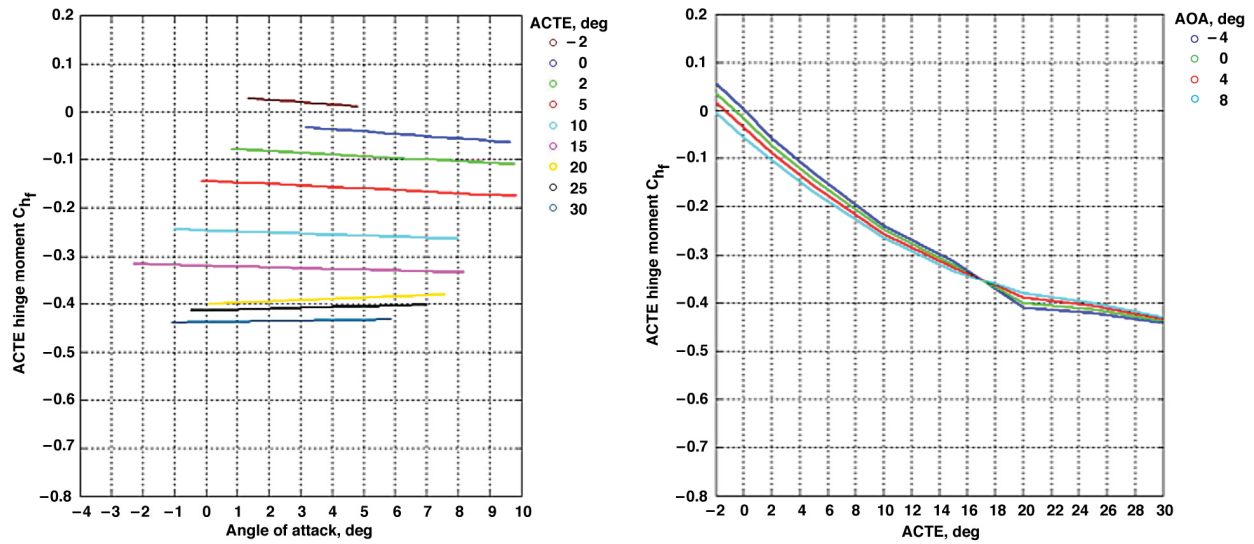


Figure 16. ACTE interface hinge moment.

### 10.3 Wing deflection measurement system

The wing deflection was measured during the ACTE flights using a single camera located in the GIII cabin that was pointed out over the left wing. Targets were located on the wing forward spar, aft spar, and the 40% chord line at five wing span stations. The camera captured one photograph every second. Average error magnitudes are less than .112 inches. The automatic detection algorithms were able to detect target locations at least 99.6% of the time or better given the various lighting effects encountered over a given flight. Figure 17 shows a photograph taken during takeoff with an overlay of the wing deflection translation from zero fuel wing jig shape. The red lines are proportional to the deflection of the wing.



Figure 17. GIII wing deflection measurement system.



## 11. ENVELOPE EXPANSION APPROACH

The envelope expansion plan consisted of incrementally expanding the envelope in small increments to safely manage any issues that may arise and build understanding regarding structure behavior. The flight testing of the flap was executed by building up in flap deflection and dynamic pressure. The ACTE project elected to start with the zero-degree flap deflection because the external pressure loads are minimal.

The load monitoring scheme consisted of monitoring the instrumentation that was located on direct load paths such as the interface fittings and direct load paths within the structure. Two load monitors were required for the control room monitoring and to make real-time calls if a parameter was inoperative or a load exceedance was observed. The control room accommodated up to four loads personnel. The additional loads personnel positions allowed for training opportunities.

Each flight consisted of a preflight checkout with the control room on headsets and data being telemetered. The preflight was an opportunity for the crew to push and pull on the flap and wing to verify that the instrumentation was working, and the data was as expected. The loads team would verify that the strain and loads matched FEM preflight predictions and or previous test data taken on the ground. Any discrepancies were discussed real time and determined whether the flight could continue. After the preflight checks, the aircraft taxied to the runway for takeoff.

After takeoff the pilots would perform a phasing maneuver, which consisted of a push-over-pull-up, bank to bank, and beta sweep maneuver. This phasing maneuver allowed a second opportunity to observe the instrumentation and verify that aircraft performance was as expected before pushing out in the envelope. After the phasing maneuver, the pilots would continue to the first flight condition.

Two maneuvers were requested from a loads perspective. The first was a push-over pull-up from 0.3g to 1.7g. This maneuver allowed the loads team to collect data over a large range of angle of attack. The second requested maneuver was wind-up-turns to 1.7g which allowed the loads team to collect loads on the flap over a range of angle of attack and load factors. The loads team also monitored the loads during the other discipline required maneuvers such as doublets, Steady Heading Side Slip (SHSS), and raps. During flight testing, it was observed that the maneuver loads on the flap were smaller than dynamic pressure effects. Most flight-test points targeted about 1.5g to 1.7g, and it is the author's opinion that targeting 2.0g for each maneuver would have resulted in better data and produced an overall better product.

The project allowed two days for data reduction and setting the flaps for the next flight. The data reduction became more refined as the project went on and probably required about 4 hours after every flight once the data was available. Table 4 highlights the maximum dynamic pressure and vertical acceleration value for each flap deflection. The lower flap deflections of 0° and 2° were flown over multiple flights due to the larger envelope, while the larger deflections of 10° to 30° had only one flight due to the small number of required flight conditions.

Table 4. ACTE flight condition summary table.

ACTE structures flight summary										
ACTE position		Flight date	Flight, #	Mach	Dynamic pressure, psf	Altitude, ft	Flap normal force, lb	Flap hinge moment, in-lb	Max dynamic pressure (QBAR), psf and max normal acceleration (Nz), g	
-2	Anchor	3/31/2015	32	0.30	94	10,000	248	-2000	QBAR	290.0
-2	Anchor	3/31/2015	32	0.40	162	10,000	-5	4771	Nz	1.7
-2	Anchor	4/15/2015	35	0.50	256	10,000	-310	14831		
-2	Max QBAR	4/15/2015	35	0.65	284	20,000	-358	19885		
0	Anchor	12/9/2014	18	0.30	94	10,000	419	-10197	QBAR	384.0
0	Anchor	11/6/2014	15	0.40	161	10,000	609	-13096	Nz	1.8
0	Anchor	12/9/2014	18	0.50	261	10,000	639	-14828		
0	Max Mach	12/9/2014	18	0.75	354	21,200	931	-19498		
0	Max QBAR	12/9/2014	18	0.60	371	10,000	600	-17402		
2	Anchor	12/18/2014	20	0.30	92	10,000	1216	-19630	QBAR	372.0
2	Anchor	12/15/2014	19	0.40	163	10,000	1561	-29728	Nz	1.8
2	Anchor	1/13/2015	21	0.50	255	10,000	1997	-44686		
2	Max Mach	1/13/2015	21	0.75	354	21,200	2989	-68120		
2	Max QBAR	1/13/2015	21	0.60	366	10,000	2474	-62182		
5	Anchor	1/22/2015	23	0.30	92	10,000	1807	-33432	QBAR	305.0
5	Anchor	3/25/2015	31	0.40	174	10,000	2503	-52777	Nz	2.0
5	Anchor	3/25/2015	31	0.50	246	10,000	3168	-72994		
5	Max Mach	3/25/2015	31	0.75	240	30,000	4157	-82584		
5	Max QBAR	3/25/2015	31	0.65	287	20,000	4127	-87678		
10	Anchor	2/4/2015	24	0.30	91	10,000	2652	-51991	QBAR	210.0
10	Anchor	2/4/2015	24	0.40	167	10,000	4134	-88845	Nz	1.8
10	Max QBAR	2/4/2015	24	0.55	200	20,000	5246	-111194		
15	Anchor	2/18/2015	26	0.30	90	10,000	3362	-67375	QBAR	210.0
15	Anchor	2/18/2015	26	0.40	169	10,000	5672	-120802	Nz	1.7
15	Max QBAR	2/18/2015	26	0.55	200	20,000	6883	-145069		
20	Anchor	3/3/2015	28	0.30	90	10,000	3920	-79019	QBAR	103.0
20	Max QBAR	3/3/2015	28	0.38	94	20,000	4172	-82810	Nz	1.7
25	Anchor	3/12/2015	29	0.30	94	10,000	4183	-83375	QBAR	100.0
25	Max QBAR	3/12/2015	29	0.38	95	20,000	4432	-88067	Nz	1.8
30	Anchor	4/22/2015	36	0.30	93	10,000	4451	-88907	QBAR	101.0
30	Max QBAR	4/22/2015	36	0.38	95	20,000	4744	-93781	Nz	1.7

## **12. HEALTH MONITORING APPROACH**

The flap health was monitored pre-and post-flight. This monitoring of the flap health was accomplished through four methods. The first method utilized the loads and strain data on the flap to verify that the loads and strains returned to the pre-flight condition. Any anomaly with the structure should show up with an offset in the loads and strain sensors. An offset in the strain gages would have required the project to further investigate the issue using non-destructive inspection methods. Having to inspect due to an offset in the strain gages never became an issue, and as the team gained more experience the trends were easily tracked.

Second, the project also visually inspected the flap for cracks, wear, and loose fasteners. Locations with little access were bore scoped to verify that there was no damage. The visual inspections were very thorough, and only minor operational issues were identified throughout the flight phase. Any anomaly found during the visual inspection could have called for additional non-destructive inspection (NDI) of the flap. The only load exceedance that occurred during the flight phase was a rudder/vertical tail load exceedance during a doublet maneuver. The flight was terminated and the vertical tail was visually inspected. No structural anomalies were identified.

The third method of health monitoring was in the pre-and post-flight laser scanning of the flap. A three-dimensional scanner was procured before the flights that could capture an accurate three-dimensional image of the flap and wing surrounding structure. This pre- and post-flight scan verified that the structure returned to its original shape after each flight.

Lastly, the accelerometer sensors were evaluated pre and post flight as way to monitor any structural changes to the flap in-flight. Overall, the project team had a good sense for the health of the structure as the flight envelope was expanded.

## **13. CONCLUSION**

The ACTE technology was flight-tested on a GIII airplane for flap deflections of  $-2^{\circ}$  up and  $+30^{\circ}$  down. The airworthiness approach to show the flap ready for flight included analysis, ground testing, instrumentation monitoring, and periodic inspections. The envelope was expanded in an incremental build-up approach to incrementally expose the project to increasing levels of manageable risk. The data collected from the flights is presented for the various flap deflections, and conclusions were drawn. The project overall was considered a success, but numerous lessons learned were captured and presented that can be applied to future flight experiments of this nature.

## **14. ACKNOWLEDGMENTS**

The authors gratefully acknowledge the work performed by Dan Goodrick in the implementation of the wing deflection measurement system. The system will aid in the future analysis work on the SCRAT Gulfstream III aircraft and future AFRC research aircraft. As well, the authors extend thanks to everyone in the Flight Loads Laboratory who assisted with the ACTE instrumentation installation and calibration of the GIII wing and interface fittings.

## 15. REFERENCES

1. Baumann, E., Hernandez, J., and Ruhf, J., “An Overview of NASA’s Subsonic Research Aircraft Testbed (SCRAT),” AIAA-2013-5083, 2013.
2. Sridhar, K., Osborn, R., Ervin, G., Dragan, M., Flick, P., and Paul, D., “Mission Adaptive Compliant Wing – Design, Fabrication and Flight Test,” *Symposium on Morphing Vehicles*, RTO-MP-AVT-168, Lisbon, Portugal, 2009, p. 18-1.
3. Gilyard, G., and Espana, M., “On the Use of Controls for Subsonic Transport Performance Improvement: Overview and Future Directions,” NASA Dryden Flight Research Center, NASA TM-4605, 1994.
4. Kota, S., “Shape-Shifting Things to Come,” *Scientific American*, Vol. 310, No. 5, pp. 58-65, May 2014.
5. Hetrick, J. A., Osborn, R. F., Kota, S., Flick, P. M., and Paul, D. B., “Flight Testing of Mission Adaptive Compliant Wing,” AIAA 2007-1709, 2007.
6. CMARC, Personal Simulation Works, <http://www.aerologic.com/>, accessed August 3, 2015.
7. TRANAIR++, CALMAR Research Corporation, <http://www.calmarresearch.com/NF/STG/Tranair/Tranair.htm>, accessed August 3, 2015.
8. MSC NASTRAN, MacNeal-Schwendler Corporation, <http://www.mscsoftware.com/product/msc-nastran>, accessed, August 3, 2015.
9. ANSYS Structural Analysis Software, ANSYS Inc., <http://www.ansys.com/?gclid=CNic5Cb13cYCFYM9aQodmP8MRA>, accessed August 3, 2015.
10. Lokos, W. A., Miller, E. J., Hudson, L. D., Holguin, A. C., Neufeld, D. C., and Haraguchi, R., “Strain Gage Loads Calibration Testing With Air Bag Support for the Gulfstream III SCRAT Aircraft,” AIAA-2015-2020, 2015.
11. Miller, E. J., Holguin, A. C., Cruz, J., and Lokos, W. A., “Strain Gage Load Calibration of the Wing Interface Fittings for the Adaptive Compliant Trailing Edge Flap Flight Test,” AIAA-2014-0277, 2014.

## 16. BIOGRAPHY

Eric Miller is the Lead Static Structures Engineer for the Adaptive Compliant Trailing Edge (ACTE) experiment at the NASA Armstrong Flight Research Center on Edwards AFB, California. His expertise includes ground proof load testing, strain gage load calibration testing, static structures flight testing, and finite element analysis. Previous ground test projects include the Global Observer wing proof loads testing and Gulfstream III wing strain gage loads calibration testing. Eric has also worked multiple NASA flight-test projects on the F-15B testbed, SOFIA Boeing 747 aircraft, and Gulfstream III testbed aircraft.